diversity

MDPI

Article

Full-Length Transcriptome Comparison Provides Novel Insights into the Molecular Basis of Adaptation to Different Ecological Niches of the Deep-Sea Hydrothermal Vent in Alvinocaridid Shrimps

Aiyang Wang [1,2,3,4], Zhongli Sha [1,2,3,4,*] and Min Hui [1,2,*]

1 Department of Marine Organism Taxonomy & Phylogeny, Institute of Oceanology, Chinese Academy of Sciences, Qingdao 266071, China; wangaiyang@qdio.ac.cn
2 Laboratory for Marine Biology and Biotechnology, Qingdao National Laboratory for Marine Science and Technology, Qingdao 266237, China
3 Shandong Province Key Laboratory of Experimental Marine Biology, Institute of Oceanology, Chinese Academy of Sciences, Qingdao 266071, China
4 University of Chinese Academy of Sciences, Beijing 100049, China
* Correspondence: shazl@qdio.ac.cn (Z.S.); minhui@qdio.ac.cn (M.H.)

Abstract: The deep-sea hydrothermal vent ecosystem is one of the extreme chemoautotrophic environments. *Shinkaicaris leurokolos* Kikuchi and Hashimoto, 2000, and *Alvinocaris longirostris* Kikuchi and Ohta, 1995, are typically co-distributed and closely related alvinocaridid shrimps in hydrothermal vent areas with different ecological niches, providing an excellent model for studying the adaptive evolution mechanism of animals in the extreme deep-sea hydrothermal vent environment. The shrimp *S. leurokolos* lives in close proximity to the chimney vent discharging high-temperature fluid, while *A. longirostris* inhabits the peripheral areas of hydrothermal vents. In this study, full-length transcriptomes of *S. leurokolos* and *A. longirostris* were generated using a combination of single-molecule real-time (SMRT) and Illumina RNA-seq technology. Expression analyses of the transcriptomes showed that among the top 30% of highly expressed genes of each species, more genes related to sulfide and heavy metal metabolism (*sulfide: quinone oxidoreductase*, *SQR*; *persulfide dioxygenase*, *ETHE1*; *thiosulfate sulfurtransferase*, *TST*, and *ferritin*, *FRI*) were specifically highly expressed in *S. leurokolos*, while genes involved in maintaining epibiotic bacteria or pathogen resistance (*beta-1,3-glucan-binding protein*, *BGBP*; *endochitinase*, *CHIT*; *acidic mammalian chitinase*, *CHIA*, and *anti-lipopolysaccharide factors*, *ALPS*) were highly expressed in *A. longirostris*. Gene family expansion analysis revealed that genes related to anti-oxidant metabolism (*cytosolic manganese superoxide dismutase*, *SODM*; *glutathione S-transferase*, *GST*, and *glutathione peroxidase*, *GPX*) and heat stress (heat shock cognate 70 kDa protein, *HSP70* and *heat shock 70 kDa protein cognate 4*, *HSP7D*) underwent significant expansion in *S. leurokolos*, while *CHIA* and *CHIT* involved in pathogen resistance significantly expanded in *A. longirostris*. Finally, 66 positively selected genes (PSGs) were identified in the vent shrimp *S. leurokolos*. Most of the PSGs were involved in DNA repair, antioxidation, immune defense, and heat stress response, suggesting their function in the adaptive evolution of species inhabiting the extreme vent microhabitat. This study provides abundant genetic resources for deep-sea invertebrates, and is expected to lay the foundation for deep decipherment of the adaptive evolution mechanism of shrimps in a deep-sea chemosynthetic ecosystem based on further whole-genome comparison.

Keywords: Alvinocarididae; adaptive evolution; deep-sea chemosynthetic ecosystem; ecological niches; full-length transcriptome

Citation: Wang, A.; Sha, Z.; Hui, M. Full-Length Transcriptome Comparison Provides Novel Insights into the Molecular Basis of Adaptation to Different Ecological Niches of the Deep-Sea Hydrothermal Vent in Alvinocaridid Shrimps. *Diversity* **2022**, *14*, 371. https://doi.org/10.3390/d14050371

Academic Editor: Michael Wink

Received: 17 April 2022
Accepted: 5 May 2022
Published: 7 May 2022

1. Introduction

Deep-sea hydrothermal vents are highly dynamic chemoautotrophic ecosystems [1]. Geothermally heated vent fluid can reach a high temperature and usually contains high

levels of heavy metals, sulfide, and low dissolved O_2 [2]. Additionally, its mixing with surrounding seawater creates environmental gradients, thereby markedly affecting the biological community composition [3]. Vent animals occupy various ecological niches with different proportions of hydrothermal fluid and great thermal heterogeneity. Certain specific locations are even under highly variable and challenging conditions. For instance, the water temperature can vary from 0 to 400 °C in a centimeter [4–7]. Animals in such regions, therefore, experience a rapid shift in temperature [6,8,9].

Understanding the mechanism of how animals have adapted to variable extreme environments and evolved is one of the central issues in evolutionary biology. Many physiological, biochemical, and molecular studies have been conducted to uncover the adaptation to hypoxia, thermal change, and heavy metals in invertebrates from hydrothermal vent ecosystems [1,3,9–14]. However, these endeavors are still far from revealing the survival strategies exhaustively. Furthermore, the genetic underpinnings of evolution in faunas' response to these harsh environments remain elusive due to the lack of genomic information.

With the rapid development of sequencing technology and bioinformatics, transcriptome sequencing technology with high affordability has been widely used to explore gene resources of vent faunas. Comparative transcriptomic analyses have been performed between different deep-sea chemosynthetic species and their shallow-water relatives to understand the molecular basis of adaptation to extreme environments of macrobenthos in deep-sea chemosynthetic ecosystems, including deep-sea fish, worms, mussels, and crab [15–18]. It has been shown that genes of positive selection, rapid evolution, or expansion in deep-sea chemosynthetic species are significantly enriched in hypoxia, immune, transporter, and thermal change-related genes, such as crustins, hemoglobins, cold-inducible proteins, and solute carrier families. Nevertheless, most of the comparative transcriptomic studies have been conducted in distantly related species with vast differences in genomic architectures and body plans, and little is known about the mechanism of adaptation to different ecological niches of hydrothermal vent areas.

All species in the family Alvinocarididae are endemic to chemosynthetic ecosystems and make up the majority of decapod crustaceans in vent and seep areas [19,20]. Among them, *Shinkaicaris leurokolos*, the only species in the genus *Shinkaicaris*, lives close to high-temperature hydrothermal discharges with strong heat-tolerance [21,22] (Figure 1A). *Alvinocaris longirostris*, belonging to the genus *Alvinocaris*, is found in both vent and seep environments [23,24] and inhabits the mussel bed in the peripheral area of hydrothermal vents [22] (Figure 1C). The two shrimps can be distinguished clearly, as there is a pair of shiny spot-like organs within the cephalothorax immediately beneath the transparent carapace of *S. leurokolos* (Figure 1B), while *A. longirostris* lacks this organ in the thoracic segment [25–27] (Figure 1D). The unique organs are considered homologous to the 'dorsal eyes' of *Rimicaris* shrimps, and might function as eyes to detect low-level illumination and evolve in response to radiation associated with hydrothermal vents [10]. Notably, *S. leurokolos* and *A. longirostris* are found co-distributed in hydrothermal vent areas of the Okinawa Trough with different ecological niches [21,22]. The shrimp *S. leurokolos* inhabits the central zone (0.2–0.8 m from the vent), while *A. longirostris* mainly inhabits far away from the active chimney (>2.5 m from the vent) [28]. Given the differences of physical and chemical factors between the microenvironments that the two alvinocaridid species inhabit, the shrimps provide an excellent model for studying the adaptive evolution mechanism of animals in the extreme deep-sea hydrothermal vent environment.

Thus far, no genome assembly has been reported for alvinocaridid shrimps. The generation of single-molecule real-time (SMRT) sequencing permits the production of reads with an average length of 10 kb, which ensures the collection of full-length transcripts. Hence, to have a deeper insight into the molecular basis of adaptation to different microenvironments in deep-sea hydrothermal vent shrimps, we performed a full-length transcriptome analysis of *S. leurokolos* and *A. longirostris* collected from the hydrothermal vent of the Okinawa Trough using a combination of SMRT long-reading sequencing and Illumina short-reading

sequencing. With these datasets, our goal is to add more genetic resources of alvinocaridid shrimps to the deep-sea life database, and to elucidate the molecular basis of their adaptation to different ecological niches by comprehensive characterization of the transcriptomes, including comparison of the highly expressed genes, significantly expanded gene families, and positively selected genes.

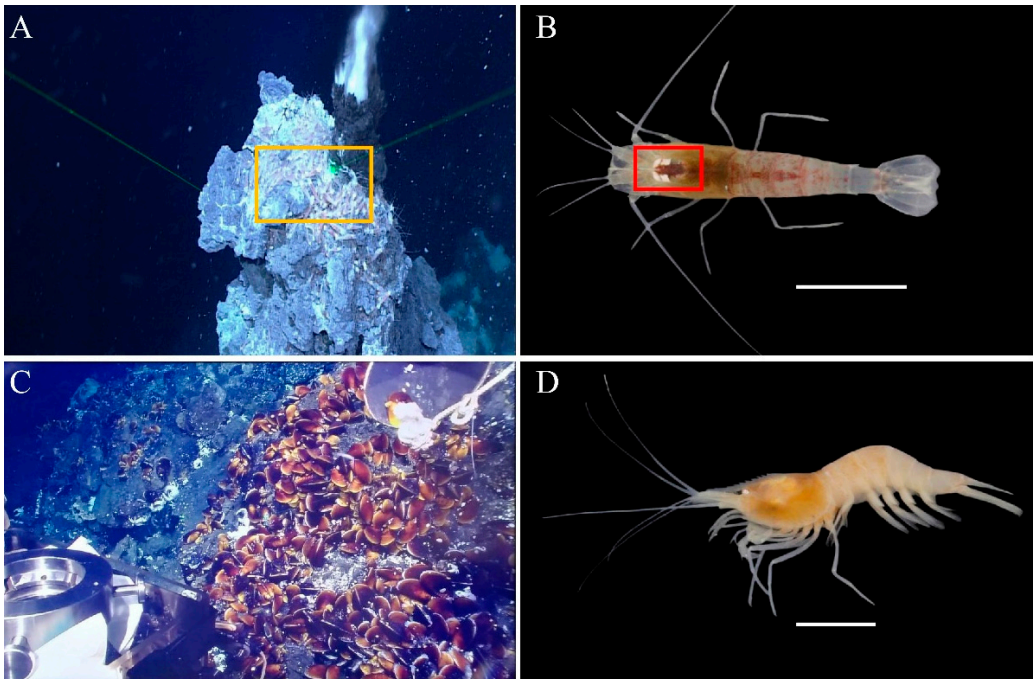

Figure 1. The in-situ living environments and morphological characteristics of the two deep-sea hydrothermal vent shrimp species. (**A**) The central zone of the Iheya North hydrothermal vent where *S. leurokolos* inhabits. *S. leurokolos* are marked in the yellow box. (**B**) Photo of *S. leurokolos* taken by Ziming Yuan. The shiny spot-like organs of *S. leurokolos* are highlighted by the red box. (**C**) The peripheral zone with the mussel bed of the Iheya North hydrothermal vent where *A. longirostris* inhabits. (**D**) Photo of *A. longirostris* taken by Ziming Yuan.

2. Materials and Methods

2.1. Sampling and RNA Extraction

Samples of *A. longirostris* and *S. leurokolos* for full-length transcriptome analysis were collected in July, 2018, while samples for Illumina short-reading sequencing were taken in April, 2014. They were all collected using the scientific research vessel (RV) KEXUE (Institute of Oceanology, Chinese Academy of Sciences, China) from the Iheya North hydrothermal vent (the depth > 1000 m) in the Okinawa Trough (126°58.50′ E, 27°32.70′ N) during the cruise by the scientific research vessel (RV) KEXUE. Samples were collected by the remotely operated vehicle (ROV) Quasar MkII on RV KEXUE and put into a thermo-maintaining bio-box. Once aboard, the samples were immediately frozen in liquid nitrogen and stored at −80 °C for RNA extraction. It should be noted that the Illumina sequencing data for *A. longirostris* used in this study was published in 2018 by Hui et al. [29].

Total RNA for the whole bodies of four *A. longirostris* (body length about 5 cm) and three *S. leurokolos* (body length about 3.2 cm) adults was extracted separately using a standard TRIzol kit (Invitrogen, Waltham, MA, USA) according to the manufacturer's instructions. The sample quality control (QC) of input total RNA was assessed by measuring the RNA Integrity Number (RIN) and concentration using an Agilent 2100 instrument, and the RNA purity was further checked through UV-spectrophotometry using a Nanodrop spectrophotometer. One of each of the RNA extractions from *A. longirostris* and *S. leurokolos* was used for SMRT sequencing. Three *A. longirostris* individuals and two *S. leurokolos* individuals were used for Illumina sequencing.

2.2. PacBio Library Construction and Sequencing

To construct PacBio Iso-Seq library, first-strand cDNA synthesis and PCR amplification were performed using the NEBNext®Single Cell/Low Input cDNA synthesis and Amplification Module combined with PacBio Iso-seq Express Oligo Kit. Next, SMRTbell™ Template Prep Kit was used to generate SMRTbell™ libraries by following the processes of DNA damage repair, end-repair, A-tailing, and ligation with Overhang Barcoded Adapters. Finally, the primers and enzymes were bound to the SMRT™ template to form a complete SMRTbell™ library. The qualified libraries were sequenced on the PacBio Sequel II System. Sequence data was processed by the SMRT Analysis software ISOseq v3.0 (with parameters: min length 50, min accuracy 0.75, min passes 1).

The reads of insert (ROI) were generated from subread BAM files. Whether the sequence contains 5′-primer, 3′-primer, and the poly-A tail categorized ROI into full-length and non-full-length sequences. Only the ROI without any adapter sequences was considered a full-length non-chimeric read. An isoform-level clustering algorithm (ICE) and a polishing program were used to obtain high-quality full-length consensus sequences with greater than 99% accuracy. Finally, any redundancy in polished consensus reads was removed by CD-HIT (c = 0.99, T = 6, G = 1, U = 10, s = 0.999, d = 40, p = 1) to obtain a final set of full length transcripts for the subsequent analysis.

2.3. Illumina Library Construction, Sequencing, and Gene Expression

The construction of Illumina RNA-seq libraries was achieved using a NEBNext® Ultra RNA library prep kit and the libraries were sequenced on an Illumina HiSeq 4000 platform following the manufacturer's instructions (Illumina, San Diego, CA, USA). Clean reads were obtained by removing the raw reads containing adapter, ploy-N (with the ratio of 'N' to be more than 10%), and low-quality reads (with a quality score less than 5). The clean reads of each library were aligned to the PacBio reference transcriptome to obtain unique mapped reads by using the Bowtie2 with mismatch 0 [30]. Fragments per kilobase of transcript per million fragments (FPKM) values showing gene expression levels were calculated by RSEM 1.2.15 software [31] with parameters -phred33-quals, -p 8, -paired-end. Unigenes in each sample were firstly sorted according to the FPKM values. The unigenes with the top 30% high FPKM values were selected for each sample of *S. leurokolos*, and then the intersection of the selected genes from all *S. leurokolos* samples was finally defined as the highly expressed genes in this shrimp species. The same procedure was processed to obtain the highly expressed genes in *A. longirostris*.

2.4. Coding Sequence Detection

TransDecoder v. 3.0.0 (https://github.com/TransDecoder, accessed on 23 March 2021) with default parameters was used to predict all transcripts' protein-coding sequences (CDS), based on the translation reading frame on the transcript sequence. The coding likelihood scores of six open reading frames (ORFs) with a length of coding protein sequences of more than 100 amino acids in a transcript were counted, and the ORF with the highest score was retained as the CDS.

2.5. Transcript Function Annotation

For functional annotation, all transcripts were annotated based on the following databases, NCBI non-redundant protein sequences (NR), NCBI non-redundant nucleotide sequences (NT), Clusters of Orthologous Groups of proteins (KOG), Swiss-Prot, Kyoto Encyclopedia of Genes and Genomes (KEGG), KEGG Ortholog databases (KO), and Gene Ontology (GO). The software of BLAST was used in NT database analysis setting the E-value threshold of 10^{-10}, while the software of Diamond BLASTX and E-value threshold of 10^{-10} were selected for NR, KOG, Swiss-Prot, and KEGG databases analysis.

2.6. Calculation of GC Content and Codon Usage

The overall GC content and codon usage of the *A. longirostris* and *S. leurokolos* full-length transcriptomes were calculated using codonW 1.4.2 (http://codonw.sourceforge.net, accessed on 8 May 2021), and the codon usage frequency was calculated with the EMBOSS CUSP program. Relative synonymous codon usage (RSCU) represented the codon usage pattern. RSCU = 1 indicated that the synonymous codon usage of the amino acid was equal and random, while RSCU < 1 and RSCU > 1 indicated negative and positive codon usage bias, respectively.

2.7. Gene Family Expansion Analysis

The protein-coding gene sequences of the other two decapods *Macrobrachium nipponense* and *Litopenaeus vannamei* were obtained from the GigaScience GigaDB database [32] and http://www.shrimpbase.net/lva.download.html (accessed on 1 June 2021), respectively. Orthologous gene families were identified for phylogenetic analysis by comparing the CDS sequences and protein sequences among *A. longirostris*, *S. leurokolos*, *M. nipponense,* and *L. vannamei*. TreeFam v8.0 pipeline (with parameters -blast_evalue $1e^{-7}$, -align_rate 0.33, -min_weight 10, -min_density 0.34, -max_size 500, -msa_method muscle) was used to define the orthologues and paralogues of the four crustaceans. In order to understand the evolutionary dynamics of genes, the size of the gene family of the most recent common ancestor was inferred with CAFE [33] based on the phylogenetic tree of the four decapods. A random birth and death process model was used to calculate the gene gains and losses of each lineage on the phylogenetic tree. The expanded gene families with a *p*-value lower than 0.01 in *S. leurokolos* were determined via comparison with the gene families in other species.

2.8. Positive Selection Analysis

To identify the genes under positive selection in *S. leurokolos*, a modified branch-site model [34] coupled with Bayesian Empirical Bayes (BEB) methods [35] was adopted to compare *S. leurokolos* with their relatives. Among *A. longirostris*, *S. leurokolos*, *M. nipponense,* and *L. vannamei*, *L. vannamei* was distantly related to the other three species, and therefore, it was removed to increase the number of single-copy orthologs.

The strength of positive selection on individual codons of each orthologue along a specifically designated lineage was estimated with the modified branch-site model using codeml program in PAML (phylogenetic analysis by maximum likelihood, v4.8) [36]. Selective pressure was evaluated by the ratio (ω) of the nonsynonymous substitution rate (dN) to the synonymous substitutions rate (dS). The ω ratio > 1 suggests positive selection, ω < 1 indicates negative selection, and ω = 1 implies neutral selection [37]. The branch-site model in PAML was used to detect positively selected genes along specific lineages with model A (model = 2 and NSsites = 2). The likelihood ratio test statistic (LRT) was performed to compare model A (fix_omega = 0) with the null model (fix_omega = 1 and omega = 1) by the codeml program. Chi-square statistically evaluated the *p*-value of LRT. The false discovery rate (FDR) method was applied to correct for multiple tests, and the threshold was set to 0.05. Moreover, the potential positive selection of specific codon sites was identified by their posterior probabilities calculated with the BEB method. Codon sites were considered under positive selection if the posterior probability value was $p \geq 0.95$.

3. Results

3.1. The Full-Length Trascripts of S. leurokolos and A. longirostris Using PacBio Sequencing

As a result, a total of 91.61 G and 80.72 G subreads, bases were generated for *S. leurokolos* and *A. longirostris*, which were archived in the Sequence Read Archive (SRA) database of NCBI with the BioProject accession number PRJNA826717. In total, 57,789,107 (*S. leurokolos*) and 48,178,061 (*A. longirostris*) polymerase reads were produced with mean passes of 45 and 43 circles and N50 length of 2180 bp and 2228 bp, respectively. After self-correction, a total of 1,059,004 and 929,230 ROIs were successfully extracted from *S.*

leurokolos and *A. longirostris*. By applying the standard Iso-Seq classification and clustering protocol, 612,807 and 389,605 full-length nonchimeric (FLNC) reads were further identified in *S. leurokolos* and *A. longirostris*. Based on the algorithm of the ICE polishing, 23,682 and 18,939 polished full-length consensus transcripts were retained in *S. leurokolos* and *A. longirostris*. After correction using short reads produced by Illumina sequencing and subsequently removing redundancy via the CD-Hit program, 16,037 and 13,666 unigenes (isoform level) with N50 length 2880 bp and 3040 bp were finally obtained for subsequent analysis in *S. leurokolos* and *A. longirostris*, respectively (Table 1). Compared with previous transcriptome studies for alvinocaridid shrimps only based on Illumina sequencing [29,38], the unigene length is greatly longer in this study of full-length transcriptomes.

Table 1. Information of Iso-Seq in *S. leurokolos* and *A. longirostris* by PacBio Sequel II platform.

Parameters	*S. leurokolos*	*A. longirostris*
Total bases	91.61 G	80.72 G
Number of polymerases reads	57,789,107	48,178,061
Polymerases reads N50 value	2180	2228
Reads of Insert (ROI)	1,059,004	929,230
Number of full-length non-chimeric reads	612,807	389,605
Number of consensus isoforms	23,682	18,939
Number of polished high-quality isoforms	23,414	18,794
Number of unigenes	16,037	13,666
Unigenes N50 length	2880 bp	3046 bp

3.2. Efficient Gene Annotation

To obtain a comprehensive functional annotation of the transcriptome, we annotated the unigenes with six databases, including NT, NR, Swiss-Prot, GO, KEGG, and KOG. The unigene sequences and their annotations of *Alvinocaris longirostris* and *Shinkaicaris leurokolos* were deposited on figshare (https://doi.org/10.6084/m9.figshare.19673844.v1, accessed on 28 April 2022). As a result, there were 11,718 and 10,243 genes in *S. leurokolos* and *A. longirostris*, respectively, annotated in at least one database. Specifically, a large portion of the unigenes (70.47 vs. 73.18%) had hits in the NR database, followed by Swissprot (59.84 vs. 60.46%) and the KOG databases (52.78 vs. 51.84%) (Table 2). In comparison with previous transcriptome studies using the second-generation sequencing technique [29,38], a higher proportion of genes have been annotated in this study, indicating the advantage of SMRT sequencing in obtaining reliable full-length transcripts.

Table 2. Summary of unigene annotation with different databases.

Annotation Database	*S. leurokolos*	*A. longirostris*
NR_Annotation	11,302 (70.47%)	10,001 (73.18%)
Swissprot_Annotation	9596 (59.84%)	8263 (60.46%)
KOG_Annotation	8465 (52.78%)	7084 (51.84%)
KEGG_Annotation	7918 (49.37%)	6717 (49.15%)
GO_Annotation	7007 (43.69%)	5720 (41.86%)
NT_Annotation	4809 (29.99%)	3561 (26.06%)
All_Annotated	11,718 (73.07%)	10,243 (74.95%)

3.3. Coding Sequence Prediction and Comparison of GC Content and Codon Usage

Analysis by TransDecoder software identified a total of 12,295 and 11,262 ORFs in *S. leurokolos* and *A. longirostris*, respectively. In *S. leurokolos*, the length of the coding proteins of the complete ORFs ranged from 100 to 2885 amino acids, while in *A. longirostris*, the length ranged from 100 to 4830 amino acids.

The GC content of the *S. leurokolos*, *A. longirostris*, and another shallow water shrimp *M. nipponense* transcriptome was 46.5, 45.8, and 50.6%, respectively. Most codons had similar proportions and RSCU values among the four species (Table S1). In *S. leurokolos*,

the proportions of amino acids were from 1.03 (Trp) to 8.12% (Leu), and in *A. longirostris*, the proportions were from 1.05 (Trp) to 8.35% (Ser). There were relatively more positively charged amino acids (13.80 vs. 13.40%) than negatively charged amino acids (13.10 vs. 12.44%) in the two deep-sea vent shrimps (Table 3). Compared with the shallow water species, the vent shrimps had a lower content of Arg, Leu, and Lys, but higher content of Phe (the difference > 1%). These changes in the amino acid composition may help enhance the adaptability of deep-sea animals to adapt to extreme environments [39–42].

Table 3. The proportions (%) of amino acid of transcriptomes from *S. leurokolos*, *A. longirostris*, and *M. nipponense*. AA: amino acid. # The differences are larger than 1% between the two deep-sea shrimps and shallow-water *M. nipponense*.

Parameters	AA	*S. leurokolos*	*A. longirostris*	*M. nipponense*
Non-polar AA	Leu #	8.12	8.28	9.55
	Ala	6.87	6.63	6.93
	Val	6.43	6.53	6.46
	Ile	4.94	4.99	4.26
	Phe #	3.44	3.54	1.49
	Met	2.42	2.35	2.04
	Trp	1.03	1.05	1.52
Polar-uncharged AA	Ser	7.94	8.35	8.81
	Gly	6.89	6.91	6.23
	Thr	6.04	6.14	5.53
	Pro	5.81	5.66	6.28
	Asn	4.17	4.33	3.40
	Gln	4.13	4.20	4.15
	Tyr	2.87	3.00	2.41
	Cys	1.81	2.01	1.70
Negative-charged AA	Glu	7.31	6.82	6.34
	Asp	5.79	5.62	5.21
Positive-charged AA	Lys #	6.18	5.74	8.03
	Arg #	5.14	5.11	7.00
	His	2.49	2.55	2.46

3.4. Highly Expressed Genes and Significantly Expanded Gene Family

In total, 93,566,442 raw reads were generated from the two *S. leurokolos* samples by Illumina sequencing. All raw reads were archived in the SRA database of NCBI with the BioProject accession number PRJNA526375. After data filtering, 13.58 G clean bases remained. The RNA-seq data for *A. longirostris* with accession number SRX3177689 (RY_A1, RY_A2, RY_A3) was from Hui et al. 2018 [29], and 22.34 G clean data for three *A. longirostris* from hydrothermal vent area were used for analysis. By mapping to the full-transcriptome, gene expression levels were determined. The number of the top 30% highly expressed genes in *S. leurokolos*, and *A. longirostris* were 3366 and 2635, respectively. The FPKM values of these genes ranged from 11.28 to 700,078.66 (average 995.79) in *S. leurokolos*, and from 13.07 to 260,318.82 (average 685.33) in *A. longirostris*.

KEGG enrichment analysis of highly expressed genes of *S. leurokolos* and *A. longirostris* was conducted to identify important pathways in adaption to their respective microenvironment in hydrothermal vents. Four KEGG pathways (antigen processing and presentation, lysosome, apoptosis, and autophagy-animal) were significantly enriched in both vent shrimps. Furthermore, pathways related to NOD-like receptor signaling pathway, sulfur metabolism, biosynthesis of amino acids, and selenocompound metabolism were specifically enriched in the top-expressed genes of *S. leurokolos* (Figure 2A), while *A. longirostris* was specifically enriched in the pathways related to oxidative phosphorylation, thermogenesis, proteasome, and phagosome (Figure 2B). The discrepancy between highly expressed genes of the two deep-sea vent shrimps may be induced by the difference of living microenvironments, such as the different temperature variation, chemoautotrophic microbes, concentrations of sulfides, methane, and heavy metals, and even food resources.

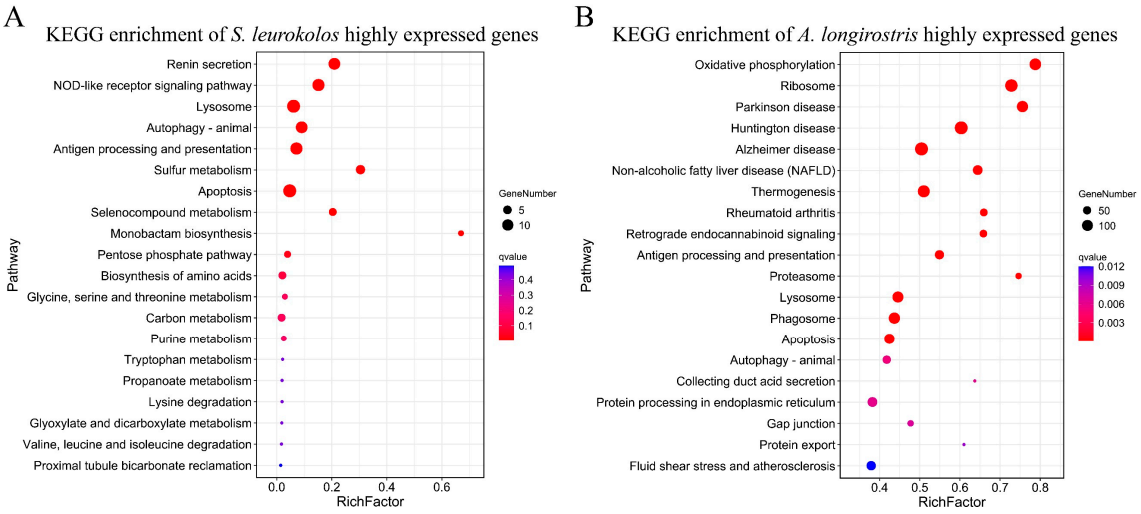

Figure 2. The 20 most enriched KEGG pathways of highly expressed genes in (**A**) *S. leurokolos* and (**B**) *A. longirostris*. "Rich factor" refers to the ratio of the highly expressed gene number and the number of genes involved in this pathway (the greater the Rich factor, the greater the degree of enrichment).The dot size is proportional to the number of enriched genes in the pathway. Red color intensity increases with enrichment significance.

Key highly expressed genes likely involved in the environmental adaptation of the two alvinocaridid species were further identified (Table S2). It was revealed that genes related to nitrogen metabolism assimilation (*glutamine synthetase*, *GLNA* and *glutamate dehydrogenase, mitochondrial*, *DHE3*) and heat and cold stress (*heat shock cognate 70 kDa protein*, *HSP70* and *cold shock Y-box protein*, *YB3*) were expressed at comparable expression levels in *S. leurokolos* and *A. longirostris*. Nevertheless, there were notable differences in the expression of several gene groups among the two species. In particular, toxic substance metabolism such as for sulfide and heavy metals (*sulfide: quinone oxidoreductase*, *SQR*; *persulfide dioxygenase*, *ETHE1*; *thiosulfate sulfurtransferase*, *TST*; and *ferritin*, *FRI*), and oxidative stress genes (*glutathione S-transferase*, *GST*; *glutathione peroxidase*, *GPX*; and *cytosolic manganese superoxide dismutase*, *SODM*) with high expression level were more abundant in *S. leurokolos* than those in *A. longirostris*, while more genes involved in immune defense (*anti-lipopolysaccharide factor*, *ALPS*; *Beta-1,3-glucan-binding protein*, *BGBP*; *endochitinase*, *CHIT*; and *acidic mammalian chitinase*, *CHIA*) were highly expressed in *A. longirostris* (Table S2).

A total of 12,809 gene families were clustered in *S. leurokolos*, *A. longirostris*, *M. nipponense*, and *L. vannamei*, of which 1103 expanded gene families (256 significant at $p < 0.01$ level) were identified in *S. leurokolos*, and 929 expanded gene families (176 significant at $p < 0.01$ level) in *A. longirostris*. It is also important to note that genes involved in oxidative stress (*SODM*, *GST*, and *GPX*) and immune responses (*CHIA* and *CHIT*) were significantly expanded mainly in *S. leurokolos* and *A. longirostris*, respectively. Furthermore, although heat stress-related genes (*HSP70* and *heat shock 70 kDa protein cognate 4*, *HSP7D*) were expressed in comparable amounts in both shrimps, we found that these genes underwent significantly expansion only in *S. leurokolos*. Interestingly, for nitrogen metabolism genes, *DHE3* significant expanded and was more highly expressed only in *S. leurokolos*, while *GLNA* significantly expanded and was more highly expressed only in *A. longirostris* (Table S3).

3.5. Positive Selection Analysis

Positive selection plays a central role in the evolution of species. To further detect genes under selection of *S. leurokolos* inhabiting the extreme vent environment, positive selection analysis has been performed. After removing *L. vannamei*, the number of single-copy putative orthologous genes of *A. longirostris*, *S. leurokolos*, and *M. nipponense* increased to 572. Of these genes, 66 positively selected genes (PSGs) were identified in *S. leurokolos* with adjusted *p*-value lower than 0.05 and BEB probability of amino acid sites larger than 0.90

(Table S4). Further analysis indicated that the PSGs included a set of genes involved in DNA repair, antioxidation, temperature stress (Table 4; Figure S1), as well as two genes related to nitrogen metabolism and transport (*sodium-dependent nutrient amino acid transporter 1*, *NAAT1* and *ammonium transporter Rh type B-B*, *RHBGB*) (Figure S1; Table S4), and a gene involved in iron homeostasis (*F-box/LRR-repeat protein 5*, *FBXL5*) (Table S4).

Table 4. Positively selected genes in *S. leurokolos* related to DNA repair, oxidative stress, and temperature stress.

Gene Name	Gene Description	Function	Adjusted *p* Value
DNA repair			
HIPK2	Homeodomain-interacting protein kinase 2	Activate DNA damage response	1.94×10^{-3}
INT6	Integrator complex subunit 6	DNA damage repair	3.73×10^{-8}
HEAT3	HEAT repeat-containing protein 3	Responding DNA damage	3.67×10^{-8}
RUVB2	RuvB-like 2	DNA damage repair	2.18×10^{-6}
SMC1A	Structural maintenance of chromosomes protein 1A	DNA damage repair	4.74×10^{-10}
SIR1	NAD-dependent protein deacetylase sirtuin-1	DNA damage repair	0.00
Oxidative stress			
CCD51	Mitochondrial potassium channel	Reduce ROS production	0.01
RT05	28S ribosomal protein S5	Reduce ROS production	7.80×10^{-5}
DHC24	Delta (24)-sterol reductase	ROS scavenging	1.45×10^{-9}
IMP2L	Mitochondrial inner membrane protease subunit 2	Regulate ROS production	0.03738529
VA0E	V-type proton ATPase subunit e	Prevent V-ATPase oxidative damage	0.006203782
Temperature stress			
PPID	Peptidyl-prolyl cis-trans isomerase D	Heat shock response	1.13×10^{-8}
EXL1	Chloride intracellular channel exl-1	Heat shock response	0.01
L2EFL	Protein lethal (2) essential for life	Heat shock response	1.85×10^{-7}
NU155	Nuclear pore complex protein Nup155	Cold shock response	9.69×10^{-8}
TCPQ	T-complex protein 1 subunit theta	Adaptation to low temperature	3.72×10^{-7}

4. Discussion

The discovery of deep-sea hydrothermal vent ecosystems greatly expanded our understanding of the limits to life on Earth [43]. The hydrothermal vent communities almost entirely depend on the emission of hydrothermal fluid, and its mixing with the water creates various surrounding environments and diverse animal compositions [44]. Therefore, there is a broad area of interest in ecology and evolution to reveal the adaptive evolution mechanisms in the closely related and co-occurring organisms in an area with different ecomorphology and niche preferences [45]. This study obtained the full-length transcriptomes of two alvinocaridid shrimps co-existing in the hydrothermal vent area of the Okinawa Through for the first time. By comprehensive characterization of the transcriptomes and comparative analysis, the molecular basis of adaptation to different ecological niches in *S. leurokolos* and *A. longirostris* has been revealed and a series of key genes involved in the adaptive process have been identified.

4.1. Temperature Adaptation

Temperature is often a critical ecological factor in determining species survival, development, behavior, and range, and thus greatly influences biogeography [46–48]. The shrimp *S. leurokolos* swarms close to the hydrothermal vents of the Okinawa Trough with drastic changes in the temperature of the surrounding seawater accompanying the eruption of hydrothermal fluid (maximum temperature higher than 300 °C) [1,22], while *A. longirostris* is relatively far from the vents, with a low water temperature of about 4 °C. Heat shock proteins, HSPs, are well-known for important roles in the stress adaptation of

decapod crustaceans, especially in response to thermal stress [49–52]. In this study, it has been found that many *HSPs* show high expression, significant expansion, and even being under positive selection, especially in *S. leurokolos*. The *HSPs* have also been identified in another alvinocaridid shrimp, *Rimicaris exoculata*, close to the vent, when they respond to heat exposure [11,53], and the expansion of *HSPs* has also been discovered in the genome of deep-sea vent and seep mussel [17]. These indicate that *HSPs* play an important role in the thermal adaptation of hydrothermal vent faunas.

Moreover, during the long-term adaptation to the thermal change near the vent, other genes related to temperature stress have also been identified as being positively selected in *S. leurokolos*, such as *protein lethal (2) essential for life* (*L2EFL*) and *nuclear pore complex protein Nup155* (*NU155*) (Table 4; Figure S1). Considering the thermal and food supply instability at hydrothermal vents, *L2EFL* may improve the ability of *S. leurokolos* to adapt to external temperature changes and starvation as reported in *Gryllus bimaculatus* [54], while *NU155* may enhance the ability of mRNA export from the nucleus to the cytoplasm after the cells are subjected to heat or cold stress [55,56]. These PSGs, probably induced by temperature constraints, might facilitate the thermoregulation of *S. leurokolos* in response to the high temperature of hydrothermal discharge.

4.2. Substance Metabolism and Detoxification

In addition to the thermal heterogeneity, the speciation and concentration of chemical elements (e.g., sulfur and heavy metals) caused by vigorous mixing of the hydrothermal fluid and ambient seawater have been suggested to play key roles in determining the composition of biological diversity [57,58]. Moreover, the spatial organization of species distribution along steep habitat environmental gradients has been proved to influence the food resource and food web structure in the deep sea [59]. The shrimp *S. leurokolos* lives in the high-stress vent habitat with low faunal richness, while *A. longirostris* inhabits a low-stress environment with high faunal richness, where there are many mussels and squat lobsters. In the specific highly expressed genes, expanded genes, and PSGs of the two vent shrimps, many substance metabolism- and detoxification-related genes have been identified, which may be driven by the particular ecological factors of their respective habitats.

The main energy sources of hydrothermal vents are chemicals from the vent fluid, such as sulfide. However, high concentrations of hydrogen sulfide will be toxic to cytochrome c oxidase systems of the aerobic respiratory organism [60,61]. As Powell and Somero have noted, vent fauna living in high sulfide environments may have mechanisms to protect their aerobic respiration from sulfide poisoning [62]. In the study, a set of genes (*SQR*, *ETHE1*, and *TST*), which can constitute a relatively complete sulfur detoxification pathway, were identified in the highly expressed gene dataset of *S. leurokolos*, in contrast to only one *TST* gene being found to be involved in sulfide metabolism among the highly expressed genes in *A. longirostris*. Among them, *SQR* encoded sulfide: quinone oxidoreductase is a critical enzyme in the first step of mitochondrial sulfide metabolism. It catalyzes toxic sulfides into polysulfides [63]. Persulfide dioxygenase (*ETHE1*, also known as *PDO*) can oxidize glutathione persulfide (GSSH) to sulfite [64], while thiosulfate sulfurtransferase (*TST*, also known as rhodanese) can convert GSSH and sulfite into thiosulfate [65]. Therefore, we hypothesize that *S. leurokolos* may enhance their sulfur detoxification capacity or utilize sulfide for inorganic energy by high expression of these sulfide metabolism-related genes, considering the limited food sources in the extreme vent environment [66].

Continuous exposure to high levels of heavy metals can poison organisms, but vent animals seem to have developed metal treatment strategies that allow them to survive in such extreme environments [67,68]. We did find that two genes, *FRI* and *MTs*, are highly expressed in both alvinocaridid shrimps, which play an important role in bioaccumulation of toxic metals and detoxification, and homeostatic regulation of metals. Specifically, *FRI* is an iron storage protein with strong ferroxidase activity [69], while *MTs* have a strong affinity for Cu, Zn, Cd, and Hg [70]. In addition, *FBXL5*, the gene encoding F-box/LRR-repeat

protein 5, is found under positive selection in *S. leurokolos*, which is an iron sensor that can regulate the intracellular iron homeostasis [71]. Therefore, these genes may play key roles in helping *S. leurokolos* and *A. longirostris* adapt to heavy metals in their environment, and some of these genes are even under selection in *S. leurokolos*, probably induced by the higher concentration of metals in the environment close to a vent.

The amino acid concentration in the hydrothermal fluid and around the hydrothermal vent communities is low and not enough to meet the organic nitrogen demand of the vent fauna [8,72]. Our data suggest that in nitrogen metabolism, *S. leurokolos* is probably more dependent on *DHE3*, while *A. longirostris* is more dependent on *GLNA*, as revealed by the gene expression and expansion data (Tables S2 and S3). Glutamine synthetase, GLNA, and glutamate dehydrogenase, DHE3, are both critical enzymes for ammonia assimilation [73]. It has been reported that GLNA can better use low-concentration ammonia, while DHE3 has better performance under high ammonia concentration [72,73]. Therefore, inorganic nitrogen concentrations near the vent and sites away from the vent might be different, and alvinocaridid shrimps may utilize these resources by regulating different genes in genomes. In addition, amino acid transporters, *NAAT1* and *RHBGB* [74–76], have been positively selected in *S. leurokolos*, which may enhance the shrimps' absorption of organic substances under the condition of food shortage.

4.3. Oxidative Stress and DNA Repair

Changes in temperature, oxygen level, and salinity may disrupt the dynamic balance of reactive oxygen species (ROS) levels and produce oxidative stress, damaging cell components and even causing cell death [77,78]. In the study, *GPX* and *GST* together making up the Glutathione antioxidant system [79], are highly expressed in the two alvinocaridid shrimps, suggesting their crucial roles in cellular defense against reactive free radicals of the extremely deep-sea chemosynthetic environment. However, these genes only expand in *S. leurokolos*, as well as *SODM* involved in scavenging superoxide radicals [80]. These suggest that *S. leurokolos* near the vent suffers much higher stress than *A. longirostris*, and therefore, these anti-oxidase related gene families expand in the adaptative evolution of *S. leurokolos*.

Moreover, the extreme deep-sea chemosynthetic environments, such as high hydrostatic pressure and high hydrogen sulfide, can cause DNA damage [81,82], and a high metal concentration can inhibit DNA repair enzymes [83]. Of the 66 positively selected genes, six are DNA repair-related genes (Table 4). Among them, homeodomain-interacting protein kinase 2 (HIPK2) is a serine/threonine kinase that phosphorylates diverse downstream targets such as the tumor suppressor p53 to activate DNA damage response and apoptosis [84–86]. Others include *Integrator complex subunit 6* (*INT6*, previously known as *DICE1*), *HEAT repeat-containing protein 3* (*HEAT3*), *RuvB-like 2* (*RUVB2*), which could perform the essential nuclear function in DNA repair [87,88] or form a complex with its homologs to participate in DNA damage repair and stress adaptation [89–91]. Structural maintenance of chromosomes protein 1A (*SMC1A*) is another PSG, which may play a role in DNA damage repair and maintaining genomic integrity [92], as well as *NAD-dependent protein deacetylase sirtuin-1* (*SIR1*) [93,94]. The positive selection of DNA repair-related genes has also been discovered in deep-sea fish [15]. Thus, *S. leurokolos* may enhance their DNA repair ability by positively selecting these genes to protect their genetic information from the destruction of the extreme central vent zone environment.

4.4. Innate Immune Response

Deep-sea hydrothermal vents are unique ecosystems sustained by chemosynthetic bacteria [95]. The hydrothermal vent shrimps always host microbes in the appendage, gill, and gut [96–98]. The relationship between the host and microbes is important for the health and even survival of these shrimps. Accompanying the differentiation of the ecological factors, the microbial diversity and distribution are linked to the characteristics of environmental gradients along with the hydrothermal chimney [99,100]. In comparison,

the habit environment of *A. longirostris* might be milder and chemically stable, which acts as an essential driving force for more prosperous microbial communities. In our study, more immune-related genes are highly expressed in *A. longirostris*, which may function in maintaining the relationship between the shrimps and their diverse microbes, or eliminate pathogens.

Among the immune related-genes, both *BGBP* and *Techylectin-5A* (*TL5A*) are pattern recognition proteins (PRPs) of crustaceans [101,102], which are highly expressed in *A. longirostris* and *S. leurokolos*, respectively. Furthermore, C-type lectins (*CTLs*) in another alvinocaridid shrimp *R. exoculata* have been revealed working in the selectivity and stability of *R. exoculata* symbionts [103]. Therefore, these highly expressed PRPs may be involved in helping *S. leurokolos* and *A. longirostris* recognize and build their unique epibiotic bacteria community [38]. Moreover, more highly expressed *ALPS* genes with broad-spectrum antimicrobial activity have been identified in *A. longirostris* compared with *S. leurokolos* (Table S2). It has been found to play an essential role in the immune defense of vent shrimps [104]. In addition, *CHIT* and *CHIA* are highly expressed and significantly expand in *A. longirostris*, which can respond to chitin-containing organisms, such as eliminating fungal pathogens and parasites [105–107]. This suggests that *A. longirostris* may interact closely with chitin-containing organisms in the environment, serving as parasites or food. In contrast, *S. leurokolos* is located in the central area of the vent, and in such a harsh environment, fewer organisms, including chitin-containing species, could survive. However, further studies into the accurate environmental factors and microbial diversities of different microenvironments, further genome comparison based on whole-genome sequencing, and in situ experiments are required to deeply reveal the adaptive mechanisms of faunas inhabiting different ecological niches of the hydrothermal vent ecosystem.

5. Conclusions

This study represents the first full-length transcriptomes of alvinocaridid shrimps specific to the chemosynthetic community. By combining PacBio SMRT- and Illumina RNA sequencing, the molecular basis of adaptation to different deep-sea hydrothermal vent ecological niches in alvinocaridid shrimps *S. leurokolos* and *A. longirostris* has been revealed comprehensively (Figure 3). In comparison, more genes related to sulfide and metal metabolisms, and antioxidation, are highly expressed in the shrimp *S. leurokolos* proximate to the vent, such as *SQR*, *GST*, and *FRI*, while more immune-related genes are highly expressed and expand in *A. longirostris* away from the vent. Different types of genes (*DHE3* and *GLNA*) encoding key enzymes in nitrogen metabolism are highly expressed and expand in the two shrimps, respectively. Gene families related to antioxidation and *HSPs* specifically expand in *S. leurokolos*. The PSGs identified in the shrimp *S. leurokolos* proximate to the vent are mainly DNA repair, temperature adaptation, and substance metabolism-related genes. These gene expression, gene family expansion, and gene sequence divergences are probably the outcome of the highly variable hydrothermal vent microenvironments, including different temperature gradients, chemical substance concentrations, and microbe communities. However, a further comparative genomic study based on whole-genome sequencing and in-situ detection of environmental factors will provide a more comprehensive explanation for the issue.

Abiotic / biotic stresses	Central zone (*Shinkaicaris leurokolos*)	Peripheral zone (*Alvinocaris longirostris*)
Temperature	Severe temperature gradient	Low
Concentration of hydrogen sulfide	High	Relatively lower
Concentration of heavey metals	High	Relatively lower
Diversity of microorganisms	Low	High

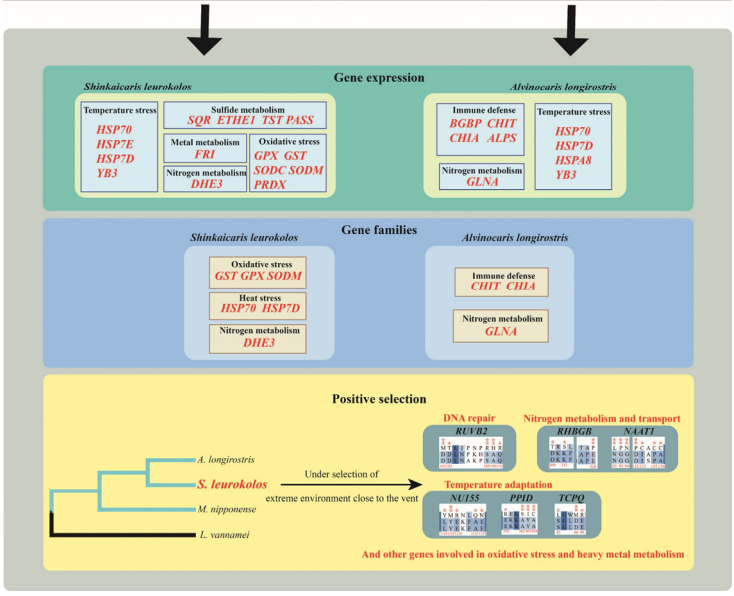

Figure 3. The outline of the molecular basis of adaptation to different ecological niches of a hydrothermal vent ecosystem in *Shinkaicaris leurokolos* and *Alvinocaris longirostris*. It depicts the main abiotic/biotic external stresses to the shrimps, and key gene sets that may play relatively important roles in the adaptation of the two shrimps to their microenvironments. Contributions of key highly expressed genes to the adaptability are described in a green square. Contributions of key significantly expanded gene families to the adaptability are described in a blue square. Finally, contributions of key positively selected genes of *S. leurokolos* to its adaptive evolution are described in a yellow square. The positive selection analysis is performed based on the phylogenetic tree of the four decapods and the orthologues of the three shrimps (branches in blue). Double asterisks stand for the amino acids in *S. leurokolos* with a BEB posterior probability that is higher than 99%, and one asterisk stands for the sites with a posterior probability larger than 95% but lower than 99%. *HSP70, heat shock cognate 70 kDa protein*; *HSP7E, heat shock 70 kDa protein cognate 5*; *HSP7D, heat shock 70 kDa protein cognate 4*; *YB3, cold shock Y-box protein*; *PAPSS, 3′-phosphoadenosine 5′-phosphosulfate synthase*; *FRI, ferritin*; *DHE3, glutamate dehydrogenase, mitochondrial*; *GPX, glutathione peroxidase*; *GST, glutathione S-transferase*; *SODC, copper/zinc superoxide dismutase*; *SODM, cytosolic manganese superoxide dismutase*; *PRDX, peroxiredoxin*; *BGBP, beta-1,3-glucan-binding protein*; *CHIT, endochitinase*; *CHIA, acidic mammalian chitinase*; *ALPS, anti-lipopolysaccharide factor*; *HSPA8, heat shock cognate 71 kDa protein*; *RUVB2, RuvB-like 2*; *RHBGB, ammonium transporter Rh type B-B*; *NAAT1, sodium-dependent nutrient amino acid transporter 1*; *NU155, nuclear pore complex protein Nup155*; *PPID, peptidyl-prolyl cis-trans isomerase D*; *TCPQ, T-complex protein 1 subunit theta*.

Supplementary Materials: The following supporting information can be downloaded at: https://www.mdpi.com/article/10.3390/d14050371/s1, Table S1: The codon usage of amino acids in *S. leurokolos*, *A. longirostris*, and *M. nipponense*; Table S2: Key highly expressed genes related to sulfide metabolism, metal metabolism, nitrogen metabolism, temperature stress, oxidative stress, and immune defense in *S. leurokolos* and *A. longirostris*; Table S3: Key significantly expanded gene family related to oxidative stress, immune defense, heat stress, and nitrogen metabolism in *S. leurokolos* and *A. longirostris*; Table S4: A complete list of positively selected genes in *S. leurokolos*; Figure S1. Partial alignment of positively selected genes (PSGs). (A) PSGs related to DNA repair. (B) PSGs related to

temperature adaptation. (C) PSGs related to nitrogen metabolism and transport. Numbers stand for the base position in the genes of *Shinkaicaris leurokolos*. Double asterisks stand for the amino acids in *S. leurokolos* with a BEB posterior probability that is higher than 99%, and one asterisk stands for the sites with a posterior probability larger than 95% but lower than 99%. Sle: *Shinkaicaris leurokolos*; Alo: *A. longirostris*; and Mni: *Macrobrachium nipponense*.

Author Contributions: A.W. analyzed the data, prepared figures and tables, authored drafts of the paper, and approved the final draft; Z.S. conceived and designed the experiments, contributed reagents and materials, reviewed drafts of the paper, and approved the final draft; M.H. conceived and designed the experiments, performed the experiments, contributed analysis tools, authored drafts of the paper, reviewed drafts of the paper, and approved the final draft. All authors have read and agreed to the published version of the manuscript.

Funding: This research was funded by the Key Deployment Project of Centre for Ocean Mega-Research of Science, Chinese Academy of Sciences (CAS), grant number COMS2019Q042, the National Natural Science Foundation of China, grant number 31872215, the Key Research Program of Frontier Sciences, CAS, grant number QYZDB-SSW-DQC036, and the National Science Foundation for Distinguished Young Scholars, grant number 42025603. The APC was funded by the National Natural Science Foundation of China, grant number 31872215.

Institutional Review Board Statement: Not applicable.

Data Availability Statement: The SMRT sequencing data for the two shrimps have been archived in the SRA database of NCBI with the BioProject accession number PRJNA826717. The Illumina data for *Shinkaicaris leurokolos* and *Alvinocaris longirostris* have been deposited in NCBI with the BioProject accession number PRJNA526375 and accession number SRX3177689, respectively. The unigene sequences and their annotations of *Alvinocaris longirostris* and *Shinkaicaris leurokolos* were deposited on figshare (https://doi.org/10.6084/m9.figshare.19673844.v1, accessed on 28 April 2022).

Acknowledgments: The samples were collected by RV KEXUE. The authors wish to thank the crews for their help during the collection of the samples.

Conflicts of Interest: The authors declare no conflict of interest.

References

1. Smith, F.; Brown, A.; Mestre, N.C.; Reed, A.J.; Thatje, S. Thermal adaptations in deep-sea hydrothermal vent and shallow-water shrimp. *Deep Sea Res. Part II Top. Stud. Oceanogr.* **2013**, *92*, 234–239. [CrossRef]
2. Little, C.T.S.; Vrijenhoek, R.C. Are hydrothermal vent animals living fossils? *Trends Ecol. Evol.* **2003**, *18*, 582–588. [CrossRef]
3. Hourdez, S.; Weber, R.E. Molecular and functional adaptations in deep-sea hemoglobins. *J. Inorg. Biochem.* **2005**, *99*, 130–141. [CrossRef] [PubMed]
4. Chevaldonné, P.; Desbruyéres, D.; Childress, J.J. . . . and some even hotter. *Nature* **1992**, *359*, 593–594. [CrossRef]
5. Delaney, J.R.; Robigou, V.; McDuff, R.E.; Tivey, M.K. Geology of a vigorous hydrothermal system on the Endeavour Segment, Juan de Fuca Ridge. *J. Geophys. Res. Solid Earth* **1992**, *97*, 19663–19682. [CrossRef]
6. Cary, S.C.; Shank, T.; Stein, J. Worms bask in extreme temperatures. *Nature* **1998**, *391*, 545–546. [CrossRef]
7. Li, L.; Du, Z.; Zhang, X.; Xi, S.; Wang, B.; Luan, Z.; Lian, C.; Yan, J. In situ Raman spectral characteristics of carbon dioxide in a deep-sea simulator of extreme environments reaching 300 °C and 30 MPa. *Appl. Spectrosc.* **2018**, *72*, 48–59. [CrossRef]
8. Johnson, K.; Childress, J.J.; Hessler, R.R.; Sakamoto-Arnold, C.M.; Beehler, C.L. Chemical and biological interactions in the Rose Garden hydrothermal vent field, Galapagos spreading center. *Deep Sea Res. Part A Oceanogr. Res. Pap.* **1988**, *35*, 1723–1744. [CrossRef]
9. McMullin, E.R.; Bergquist, D.C.; Fisher, C.R. Metazoans in extreme environments: Adaptations of hydrothermal vent and hydrocarbon seep fauna. *Gravit. Space Biol. Bull. Publ. Am. Soc. Gravit. Space Biol.* **2000**, *13*, 13–23.
10. Dover, C.L.V.; Szuts, E.Z.; Chamberlain, S.C.; Cann, J.R. A novel eye in 'eyeless' shrimp from hydrothermal vents of the Mid-Atlantic Ridge. *Nature* **1989**, *337*, 458–460. [CrossRef]
11. Ravaux, J.; Gaill, F.; Le Bris, N.; Sarradin, P.-M.; Jollivet, D.; Shillito, B. Heat-shock response and temperature resistance in the deep-sea vent shrimp *Rimicaris exoculata*. *J. Exp. Biol.* **2003**, *206*, 2345–2354. [CrossRef] [PubMed]
12. Hardivillier, Y.; Leignel, V.; Denis, F.; Uguen, G.; Cosson, R.; Laulier, M. Do organisms living around hydrothermal vent sites contain specific metallothioneins? The case of the genus *Bathymodiolus* (Bivalvia, Mytilidae). *Comp. Biochem. Physiol. Part C Toxicol. Pharmacol.* **2004**, *139*, 111–118. [CrossRef] [PubMed]
13. Hourdez, S.; Lallier, F.H. Adaptations to hypoxia in hydrothermal-vent and cold-seep invertebrates. In *Life in Extreme Environments*; Amils, R., Ellis-Evans, C., Hinghofer-Szalkay, H., Eds.; Springer: Dordrecht, The Netherlands, 2007; pp. 297–313.

14. Zeng, Z.; Ma, Y.; Wang, X.; Chen, C.-T.A.; Yin, X.; Zhang, S.; Zhang, J.; Jiang, W. Elemental compositions of crab and snail shells from the Kueishantao hydrothermal field in the southwestern Okinawa Trough. *J. Mar. Syst.* **2018**, *180*, 90–101. [CrossRef]
15. Lan, Y.; Sun, J.; Xu, T.; Chen, C.; Tian, R.; Qiu, J.-W.; Qian, P.-Y. De novo transcriptome assembly and positive selection analysis of an individual deep-sea fish. *BMC Genom.* **2018**, *19*, 394. [CrossRef]
16. Zhang, Y.; Sun, J.; Chen, C.; Watanabe, H.K.; Feng, D.; Zhang, Y.; Chiu, J.M.Y.; Qian, P.-Y.; Qiu, J.-W. Adaptation and evolution of deep-sea scale worms (Annelida: Polynoidae): Insights from transcriptome comparison with a shallow-water species. *Sci. Rep.* **2017**, *7*, 46205. [CrossRef]
17. Zheng, P.; Wang, M.; Li, C.; Sun, X.; Wang, X.; Sun, Y.; Sun, S. Insights into deep-sea adaptations and host–symbiont interactions: A comparative transcriptome study on *Bathymodiolus* mussels and their coastal relatives. *Mol. Ecol.* **2017**, *26*, 5133–5148. [CrossRef]
18. Hui, M.; Song, C.; Liu, Y.; Li, C.; Cui, Z. Exploring the molecular basis of adaptive evolution in hydrothermal vent crab *Austinograea alayseae* by transcriptome analysis. *PLoS ONE* **2017**, *12*, e0178417. [CrossRef]
19. Martin, J.W.; Haney, T.A. Decapod crustaceans from hydrothermal vents and cold seeps: A review through 2005. *Zool. J. Linn. Soc.* **2005**, *145*, 445–522. [CrossRef]
20. Yahagi, T.; Watanabe, H.; Kojima, S.; Beedessee, G.; Komai, T. First record and a new species of *Alvinocaris Williams* & Chace, 1982 (Crustacea: Decapoda: Caridea: Alvinocarididae) from the Indian Ocean. *Zootaxa* **2014**, *3893*, 101–113. [CrossRef]
21. Yahagi, T.; Watanabe, H.; Ishibashi, J.-I.; Kojima, S. Genetic population structure of four hydrothermal vent shrimp species (Alvinocarididae) in the Okinawa Trough, Northwest Pacific. *Mar. Ecol. Prog. Ser.* **2015**, *529*, 159–169. [CrossRef]
22. Miyazaki, J.; Kawagucci, S.; Makabe, A.; Takahashi, A.; Kitada, K.; Torimoto, J.; Matsui, Y.; Tasumi, E.; Shibuya, T.; Nakamura, K.; et al. Deepest and hottest hydrothermal activity in the Okinawa Trough: The Yokosuka site at Yaeyama Knoll. *R. Soc. Open Sci.* **2017**, *4*, 171570. [CrossRef] [PubMed]
23. Tokuda, G.; Yamada, A.; Nakano, K.; Arita, N.; Yamasaki, H. Occurrence and recent long-distance dispersal of deep-sea hydrothermal vent shrimps. *Biol. Lett.* **2005**, *2*, 257–260. [CrossRef] [PubMed]
24. Komai, T.; Segonzac, M. Taxonomic Review of the Hydrothermal Vent Shrimp Genera *Rimicaris* Williams & Rona and *Chorocaris* Martin & Hessler (Crustacea: Decapoda: Caridea: Alvinocarididae). *J. Shellfish Res.* **2008**, *27*, 21–41. [CrossRef]
25. Komai, T.; Segonzac, M. A revision of the genus *Alvinocaris* Williams and Chace (Crustacea: Decapoda: Caridea: Alvinocarididae), with descriptions of a new genus and a new species of *Alvinocaris*. *Ann. Mag. Nat. Hist.* **2005**, *39*, 1111–1175. [CrossRef]
26. Komai, T.; Chan, T.-Y. A new genus and two new species of alvinocaridid shrimps (Crustacea: Decapoda: Caridea) from a hydrothermal vent field off northeastern Taiwan. *Zootaxa* **2010**, *2372*, 15–32. [CrossRef]
27. Watanabe, H.; Yahagi, T.; Nagai, Y.; Seo, M.; Kojima, S.; Ishibashi, J.-I.; Yamamoto, H.; Fujikura, K.; Mitarai, S.; Toyofuku, T. Different thermal preferences for brooding and larval dispersal of two neighboring shrimps in deep-sea hydrothermal vent fields. *Mar. Ecol.* **2016**, *37*, 1282–1289. [CrossRef]
28. Watanabe, H.; Kojima, S. Vent Fauna in the Okinawa Trough. In *Subseafloor Biosphere Linked to Hydrothermal Systems: TAIGA Concept*; Ishibashi, J.-I., Okino, K., Sunamura, M., Eds.; Springer: Tokyo, Japan, 2015; pp. 449–459.
29. Hui, M.; Cheng, J.; Sha, Z. Adaptation to the deep-sea hydrothermal vents and cold seeps: Insights from the transcriptomes of *Alvinocaris longirostris* in both environments. *Deep Sea Res. Part I Oceanogr. Res. Pap.* **2018**, *135*, 23–33. [CrossRef]
30. Langmead, B.; Salzberg, S.L. Fast gapped-read alignment with Bowtie 2. *Nat. Methods* **2012**, *9*, 357–359. [CrossRef]
31. Li, B.; Dewey, C.N. RSEM: Accurate transcript quantification from RNA-Seq data with or without a reference genome. *BMC Bioinform.* **2011**, *12*, 323. [CrossRef]
32. Jin, S.; Bian, C.; Jiang, S.; Han, K.; Xiong, Y.; Zhang, W.; Shi, C.; Qiao, H.; Gao, Z.; Li, R.; et al. A chromosome-level genome assembly of the oriental river prawn, *Macrobrachium nipponense*. *GigaScience* **2021**, *10*, giaa160. [CrossRef]
33. De Bie, T.; Cristianini, N.; Demuth, J.P.; Hahn, M.W. CAFE: A computational tool for the study of gene family evolution. *Bioinformatics* **2006**, *22*, 1269–1271. [CrossRef] [PubMed]
34. Yang, Z.; dos Reis, M. Statistical Properties of the Branch-Site Test of Positive Selection. *Mol. Biol. Evol.* **2011**, *28*, 1217–1228. [CrossRef] [PubMed]
35. Yang, Z.; Wong, W.S.W.; Nielsen, R. Bayes Empirical Bayes Inference of amino acid sites under positive selection. *Mol. Biol. Evol.* **2005**, *22*, 1107–1118. [CrossRef] [PubMed]
36. Yang, Z. PAML 4: Phylogenetic Analysis by Maximum Likelihood. *Mol. Biol. Evol.* **2007**, *24*, 1586–1591. [CrossRef]
37. Yang, Z.; Nielsen, R. Codon-Substitution Models for Detecting Molecular Adaptation at Individual Sites Along Specific Lineages. *Mol. Biol. Evol.* **2002**, *19*, 908–917. [CrossRef]
38. Zhu, F.-C.; Sun, J.; Yan, G.-Y.; Huang, J.-M.; Chen, C.; He, L.-S. Insights into the strategy of micro-environmental adaptation: Transcriptomic analysis of two alvinocaridid shrimps at a hydrothermal vent. *PLoS ONE* **2020**, *15*, e0227587. [CrossRef]
39. Ayala-del-Río Héctor, L.; Chain Patrick, S.; Grzymski Joseph, J.; Ponder Monica, A.; Ivanova, N.; Bergholz Peter, W.; Di Bartolo, G.; Hauser, L.; Land, M.; Bakermans, C.; et al. The Genome Sequence of *Psychrobacter arcticus* 273-4, a Psychroactive Siberian Permafrost Bacterium, Reveals Mechanisms for Adaptation to Low-Temperature Growth. *Appl. Environ. Microbiol.* **2010**, *76*, 2304–2312. [CrossRef]
40. Zhao, J.-S.; Deng, Y.; Manno, D.; Hawari, J. *Shewanella* spp. genomic evolution for a cold marine lifestyle and in-situ explosive biodegradation. *PLoS ONE* **2010**, *5*, e9109. [CrossRef]

41. Saunders, N.F.; Thomas, T.; Curmi, P.M.; Mattick, J.S.; Kuczek, E.; Slade, R.; Davis, J.; Franzmann, P.D.; Boone, D.; Rusterholtz, K.; et al. Mechanisms of Thermal Adaptation Revealed From the Genomes of the Antarctic *Archaea Methanogenium frigidum* and *Methanococcoides burtonii*. *Genome Res.* **2003**, *13*, 1580–1588. [CrossRef]
42. Yang, L.-L.; Tang, S.-K.; Huang, Y.; Zhi, X.-Y. Low Temperature Adaptation Is Not the Opposite Process of High Temperature Adaptation in Terms of Changes in Amino Acid Composition. *Genome Biol. Evol.* **2015**, *7*, 3426–3433. [CrossRef]
43. Van Dover, C.L.; German, C.R.; Speer, K.G.; Parson, L.M.; Vrijenhoek, R.C. Evolution and Biogeography of Deep-Sea Vent and Seep Invertebrates. *Science* **2002**, *295*, 1253–1257. [CrossRef] [PubMed]
44. Cottin, D.; Ravaux, J.; Léger, N.; Halary, S.; Toullec, J.-Y.; Sarradin, P.-M.; Gaill, F.; Shillito, B. Thermal biology of the deep-sea vent annelid *Paralvinella grasslei*:in vivostudies. *J. Exp. Biol.* **2008**, *211*, 2196–2204. [CrossRef] [PubMed]
45. Davies, T.J.; Meiri, S.; Barraclough, T.G.; Gittleman, J.L. Species co-existence and character divergence across carnivores. *Ecol. Lett.* **2007**, *10*, 146–152. [CrossRef] [PubMed]
46. Somero, G.N. Linking biogeography to physiology: Evolutionary and acclimatory adjustments of thermal limits. *Front. Zool.* **2005**, *2*, 1–9. [CrossRef] [PubMed]
47. Collier, R.J.; Gebremedhin, K.G. Thermal Biology of Domestic Animals. *Annu. Rev. Anim. Biosci.* **2015**, *3*, 513–532. [CrossRef]
48. Wojda, I. Temperature stress and insect immunity. *J. Therm. Biol.* **2017**, *68*, 96–103. [CrossRef]
49. Madeira, D.; Narciso, L.; Cabral, H.N.; Diniz, M.S.; Vinagre, C. Thermal tolerance of the crab *Pachygrapsus marmoratus*: Intraspecific differences at a physiological (CTMax) and molecular level (Hsp70). *Cell Stress Chaperones* **2012**, *17*, 707–716. [CrossRef]
50. Yuan, K.; Yuan, F.-H.; He, H.-H.; Bi, H.-T.; Weng, S.-P.; He, J.-G.; Chen, Y.-H. Heat shock 70 kDa protein cognate 5 involved in WSSV toleration of *Litopenaeus vannamei*. *Dev. Comp. Immunol.* **2017**, *72*, 9–20. [CrossRef]
51. Liu, Z.-M.; Zhu, X.-L.; Lu, J.; Cai, W.-J.; Ye, Y.-P.; Lv, Y.-P. Effect of high temperature stress on heat shock protein expression and antioxidant enzyme activity of two morphs of the mud crab *Scylla paramamosain*. *Comp. Biochem. Physiol. Part A Mol. Integr. Physiol.* **2018**, *223*, 10–17. [CrossRef]
52. Sornchuer, P.; Junprung, W.; Yingsunthonwattana, W.; Tassanakajon, A. Heat shock factor 1 regulates heat shock proteins and immune-related genes in *Penaeus monodon* under thermal stress. *Dev. Comp. Immunol.* **2018**, *88*, 19–27. [CrossRef] [PubMed]
53. Cottin, D.; Shillito, B.; Chertemps, T.; Thatje, S.; Léger, N.; Ravaux, J. Comparison of heat-shock responses between the hydrothermal vent shrimp *Rimicaris exoculata* and the related coastal shrimp *Palaemonetes varians*. *J. Exp. Mar. Biol. Ecol.* **2010**, *393*, 9–16. [CrossRef]
54. Kwon, K.; Lee, N.; Yu, K.O. Lethal (2) Essential for Life l(2)efl Gene in the Two-spotted Cricket, *Gryllus bimaculatus* (Orthoptera: Gryllidae). *J. Life Sci.* **2021**, *31*, 671–676. [CrossRef]
55. Rollenhagen, C.; Hodge, C.A.; Cole, C.N. The Nuclear Pore Complex and the DEAD Box Protein Rat8p/Dbp5p Have Nonessential Features Which Appear To Facilitate mRNA Export following Heat Shock. *Mol. Cell. Biol.* **2004**, *24*, 4869–4879. [CrossRef] [PubMed]
56. Qian, B.; Xue, L. Liver transcriptome sequencing and de novo annotation of the large yellow croaker (*Larimichthy crocea*) under heat and cold stress. *Mar. Genom.* **2016**, *25*, 95–102. [CrossRef]
57. Johnson, K.S.; Beehler, C.L.; Sakamoto-Arnold, C.M.; Childress, J.J. In Situ Measurements of Chemical Distributions in a Deep-Sea Hydrothermal Vent Field. *Science* **1986**, *231*, 1139–1141. [CrossRef]
58. Luther, G.W.; Rozan, T.F.; Taillefert, M.; Nuzzio, D.B.; Di Meo, C.; Shank, T.M.; Lutz, R.A.; Cary, S.C. Chemical speciation drives hydrothermal vent ecology. *Nature* **2001**, *410*, 813–816. [CrossRef]
59. Levesque, C.; Juniper, S.K.; Limén, H. Spatial organization of food webs along habitat gradients at deep-sea hydrothermal vents on Axial Volcano, Northeast Pacific. *Deep Sea Res. Part I Oceanogr. Res. Pap.* **2006**, *53*, 726–739. [CrossRef]
60. Tunnicliffe, V. The biology of hydrothermal vents: Ecology and evolution. *Oceanog. Mar. Biol.* **1991**, *29*, 319–407.
61. Compère, P.; Martinez, A.-S.; Charmantier-Daures, M.; Toullec, J.-Y.; Goffinet, G.; Gaill, F. Does sulphide detoxication occur in the gills of the hydrothermal vent shrimp, *Rimicaris exoculata*? *Comptes Rendus. Biol.* **2002**, *325*, 591–596. [CrossRef]
62. Powell, M.A.; Somero, G.N. Adaptations to sulfide by hydrothermal vent animals: Sites and mechanisms of detoxification and metabolism. *Biol. Bull.* **1986**, *171*, 274–290. [CrossRef]
63. Xin, Y.; Liu, H.; Cui, F.; Liu, H.; Xun, L. Recombinant *Escherichia coli* with sulfide:quinone oxidoreductase and persulfide dioxygenase rapidly oxidises sulfide to sulfite and thiosulfate via a new pathway. *Environ. Microbiol.* **2016**, *18*, 5123–5136. [CrossRef] [PubMed]
64. Liu, H.; Xin, Y.; Xun, L. Distribution, Diversity, and Activities of Sulfur Dioxygenases in Heterotrophic Bacteria. *Appl. Environ. Microbiol.* **2014**, *80*, 1799–1806. [CrossRef] [PubMed]
65. Hildebrandt, T.M.; Grieshaber, M.K. Three enzymatic activities catalyze the oxidation of sulfide to thiosulfate in mammalian and invertebrate mitochondria. *FEBS J.* **2008**, *275*, 3352–3361. [CrossRef] [PubMed]
66. Doeller, J.E.; Grieshaber, M.K.; Kraus, D.W. Chemolithoheterotrophy in a metazoan tissue: Thiosulfate production matches ATP demand in ciliated mussel gills. *J. Exp. Biol.* **2001**, *204*, 3755–3764. [CrossRef]
67. Cosson, R.P.; Thiébaut, E.; Company, R.; Castrec-Rouelle, M.; Colaço, A.; Martins, I.; Sarradin, P.-M.; Bebianno, M.J. Spatial variation of metal bioaccumulation in the hydrothermal vent mussel *Bathymodiolus azoricus*. *Mar. Environ. Res.* **2008**, *65*, 405–415. [CrossRef]
68. Kádár, E.; Costa, V.; Santos, R.S. Distribution of micro-essential (Fe, Cu, Zn) and toxic (Hg) metals in tissues of two nutritionally distinct hydrothermal shrimps. *Sci. Total Environ.* **2006**, *358*, 143–150. [CrossRef]

69. Liu, X.-L.; Ye, S.; Li, H.-W.; Lu, B.; Yu, Y.-Q.; Fan, Y.-P.; Yang, W.-J.; Yang, J.-S. An H-ferritin from the hydrothermal vent shrimp *Rimicaris exoculata* and its potential role in iron metabolism. *BioMetals* **2019**, *32*, 251–264. [CrossRef]
70. Mao, H.; Wang, D.-H.; Yang, W.-X. The involvement of metallothionein in the development of aquatic invertebrate. *Aquat. Toxicol.* **2012**, *110*, 208–213. [CrossRef]
71. Alvarez-Carreño, C.; Alva, V.; Becerra, A.; Lazcano, A. Structure, function and evolution of the hemerythrin-like domain superfamily. *Protein Sci.* **2018**, *27*, 848–860. [CrossRef]
72. Lee, R.W.; Robinson, J.J.; Cavanaugh, C.M. Pathways of inorganic nitrogen assimilation in chemoautotrophic bacteria-marine invertebrate symbioses: Expression of host and symbiont glutamine synthetase. *J. Exp. Biol.* **1999**, *202*, 289–300. [CrossRef]
73. Reitzer, L.J. Ammonia assimilation and the biosynthesis of glutamine, glutamate, aspartate, asparagine, L-alanine and D-alanine. In *Escherichia coli and Salmonella typhimurium:Cellular and Molecular Biology*; American Society for Microbiology: Washington, DC, USA, 1987; pp. 302–320.
74. Fu, K.-Y.; Guo, W.-C.; Ahmat, T.; Li, G.-Q. Knockdown of a nutrient amino acid transporter gene *LdNAT1* reduces free neutral amino acid contents and impairs *Leptinotarsa decemlineata* pupation. *Sci. Rep.* **2015**, *5*, 18124. [CrossRef] [PubMed]
75. Mirandela, G.D.; Tamburrino, G.; Hoskisson, P.A.; Zachariae, U.; Javelle, A. The lipid environment determines the activity of the *Escherichia coli* ammonium transporter AmtB. *FASEB J.* **2019**, *33*, 1989–1999. [CrossRef] [PubMed]
76. Soupene, E.; Inwood, W.; Kustu, S. Lack of the Rhesus protein Rh1 impairs growth of the green alga *Chlamydomonas reinhardtii* at high CO_2. *Proc. Natl. Acad. Sci. USA* **2004**, *101*, 7787–7792. [CrossRef] [PubMed]
77. Lushchak, V.I. Environmentally induced oxidative stress in aquatic animals. *Aquat. Toxicol.* **2011**, *101*, 13–30. [CrossRef]
78. Sharma, P.; Jha, A.B.; Dubey, R.S.; Pessarakli, M. Reactive Oxygen Species, Oxidative Damage, and Antioxidative Defense Mechanism in Plants under Stressful Conditions. *J. Bot.* **2012**, *2012*, 217037. [CrossRef]
79. Duan, Y.; Liu, P.; Li, J.; Li, J.; Chen, P. Expression profiles of selenium dependent glutathione peroxidase and glutathione S-transferase from *Exopalaemon carinicauda* in response to *Vibrio anguillarum* and WSSV challenge. *Fish Shellfish Immunol.* **2013**, *35*, 661–670. [CrossRef]
80. Gomezanduro, G.; Barillasmury, C.; Peregrino-Uriarte, A.B.; Gupta, L.; Gollasgalvan, T.; Hernandezlopez, J.; Yepizplascencia, G. The cytosolic manganese superoxide dismutase from the shrimp *Litopenaeus vannamei*: Molecular cloning and expression. *Dev. Comp. Immunol.* **2006**, *30*, 893–900. [CrossRef]
81. Aertsen, A.; Van Houdt, R.; Vanoirbeek, K.; Michiels, C.W. An SOS Response Induced by High Pressure in *Escherichia coli*. *J. Bacteriol.* **2004**, *186*, 6133–6141. [CrossRef]
82. Rothschild, L.J.; Mancinelli, R.L. Life in extreme environments. *Nature* **2001**, *409*, 1092–1101. [CrossRef]
83. Hartwig, A. Carcinogenicity of metal compounds: Possible role of DNA repair inhibition. *Toxicol. Lett.* **1998**, *102*, 235–239. [CrossRef]
84. D'Orazi, G.; Cecchinelli, B.; Bruno, T.; Manni, I.; Higashimoto, Y.; Saito, S.; Gostissa, M.; Coen, S.; Marchetti, A.; Del Sal, G.; et al. Homeodomain-interacting protein kinase-2 phosphorylates p53 at Ser 46 and mediates apoptosis. *Nat. Cell Biol.* **2001**, *4*, 11–19. [CrossRef] [PubMed]
85. Kuwano, Y.; Nishida, K.; Akaike, Y.; Kurokawa, K.; Nishikawa, T.; Masuda, K.; Rokutan, K. Homeodomain-Interacting Protein Kinase-2: A Critical Regulator of the DNA Damage Response and the Epigenome. *Int. J. Mol. Sci.* **2016**, *17*, 1638. [CrossRef] [PubMed]
86. Reuven, N.; Adler, J.; Porat, Z.; Polonio-Vallon, T.; Hofmann, T.G.; Shaul, Y. The Tyrosine Kinase c-Abl Promotes Homeodomain-interacting Protein Kinase 2 (HIPK2) Accumulation and Activation in Response to DNA Damage. *J. Biol. Chem.* **2015**, *290*, 16478–16488. [CrossRef]
87. Wieland, I.; Arden, K.C.; Michels, D.; Klein-Hitpass, L.; Böhm, M.; Viars, C.S.; Weidle, U.H. Isolation of DICE1: A gene frequently affected by LOH and downregulated in lung carcinomas. *Oncogene* **1999**, *18*, 4530–4537. [CrossRef] [PubMed]
88. Wieland, I.; Röpke, A.; Stumm, M.; Sell, C.; Weidle, U.; Wieacker, P. Molecular Characterization of the DICE1 (DDX26) Tumor Suppressor Gene in Lung Carcinoma Cells. *Oncol. Res. Featur. Preclin. Clin. Cancer Ther.* **2001**, *12*, 491–500. [CrossRef]
89. Hannan, K.M.; Soo, P.; Wong, M.S.; Lee, J.K.; Hein, N.; Evers, M.; Wysoke, K.D.; Williams, T.D.; Montellese, C.; Smith, L.K.; et al. Nuclear stabilisation of p53 requires a functional nucleolar surveillance pathway. *bioRxiv* **2021**. [CrossRef]
90. Jha, S.; Dutta, A. RVB1/RVB2: Running Rings around Molecular Biology. *Mol. Cell* **2009**, *34*, 521–533. [CrossRef]
91. Nano, N.; Houry, W.A. Chaperone-like activity of the AAA+ proteins Rvb1 and Rvb2 in the assembly of various complexes. *Philos. Trans. R. Soc. B Biol. Sci.* **2013**, *368*, 20110399. [CrossRef]
92. Yi, F.; Wang, Z.; Liu, J.; Zhang, Y.; Wang, Z.; Xu, H.; Li, X.; Bai, N.; Cao, L.; Song, X. Structural Maintenance of Chromosomes protein 1: Role in Genome Stability and Tumorigenesis. *Int. J. Biol. Sci.* **2017**, *13*, 1092–1099. [CrossRef]
93. Langsfeld, E.S.; Bodily, J.; Laimins, L.A. The Deacetylase Sirtuin 1 Regulates Human Papillomavirus Replication by Modulating Histone Acetylation and Recruitment of DNA Damage Factors NBS1 and Rad51 to Viral Genomes. *PLoS Pathog.* **2015**, *11*, e1005181. [CrossRef]
94. Terauchi, K.; Kobayashi, H.; Yatabe, K.; Yui, N.; Fujiya, H.; Niki, H.; Musha, H.; Yudoh, K. The NAD-Dependent Deacetylase Sirtuin-1 Regulates the Expression of Osteogenic Transcriptional Activator Runt-Related Transcription Factor 2 (Runx2) and Production of Matrix Metalloproteinase (MMP)-13 in Chondrocytes in Osteoarthritis. *Int. J. Mol. Sci.* **2016**, *17*, 1019. [CrossRef] [PubMed]

95. Van Dover, C.L.; Lutz, R.A. Experimental ecology at deep-sea hydrothermal vents: A perspective. *J. Exp. Mar. Biol. Ecol.* **2004**, *300*, 273–307. [CrossRef]
96. Tokuda, G.; Yamada, A.; Nakano, K.; Arita, N.O.; Yamasaki, H. Colonization of *Sulfurovum* sp. on the gill surfaces of *Alvinocaris longirostris*, a deep-sea hydrothermal vent shrimp. *Mar. Ecol.* **2008**, *29*, 106–114. [CrossRef]
97. Petersen, J.M.; Ramette, A.; Lott, C.; Cambon-Bonavita, M.-A.; Zbinden, M.; Dubilier, N. Dual symbiosis of the vent shrimp *Rimicaris exoculata* with filamentous gamma- and epsilonproteobacteria at four Mid-Atlantic Ridge hydrothermal vent fields. *Environ. Microbiol.* **2010**, *12*, 2204–2218. [CrossRef] [PubMed]
98. Sun, Q.-l.; Zeng, Z.-g.; Chen, S.; Sun, L. First comparative analysis of the community structures and carbon metabolic pathways of the bacteria associated with *Alvinocaris longirostris* in a hydrothermal vent of okinawa trough. *PLoS ONE* **2016**, *11*, e0154359. [CrossRef]
99. Sievert, S.; Brinkhoff, T.; Muyzer, G.; Ziebis, W.; Kuever, J. Spatial Heterogeneity of Bacterial Populations along an Environmental Gradient at a Shallow Submarine Hydrothermal Vent near Milos Island (Greece). *Appl. Environ. Microbiol.* **1999**, *65*, 3834–3842. [CrossRef]
100. Pagé, A.; Tivey, M.K.; Stakes, D.S.; Reysenbach, A.-L. Temporal and spatial archaeal colonization of hydrothermal vent deposits. *Environ. Microbiol.* **2008**, *10*, 874–884. [CrossRef]
101. Goncalves, P.; Vernal, J.; Rosa, R.D.; Yepiz-Plascencia, G.; de Souza, C.; Barracco, M.A.; Perazzolo, L.M. Evidence for a novel biological role for the multifunctional β-1,3-glucan binding protein in shrimp. *Mol. Immunol.* **2012**, *51*, 363–367. [CrossRef]
102. Kawabata, S.; Beisel, H.G.; Huber, R.; Bode, W.; Gokudan, S.; Muta, T.; Tsuda, R.; Koori, K.; Kawahara, T.; Seki, N.; et al. Role of tachylectins in host defense of the Japanese horseshoe crab *Tachypleus Tridentatus*. In *Phylogenetic Perspectives on the Vertebrate Immune System*; Beck, G., Sugumaran, M., Cooper, E.L., Eds.; Springer: Boston, MA, USA, 2001; pp. 195–202.
103. Liu, X.-L.; Ye, S.; Cheng, C.-Y.; Li, H.-W.; Lu, B.; Yang, W.-J.; Yang, J.-S. Identification and characterization of a symbiotic agglutination-related C-type lectin from the hydrothermal vent shrimp *Rimicaris exoculata*. *Fish Shellfish Immunol.* **2019**, *92*, 1–10. [CrossRef]
104. Gu, H.-j.; Sun, Q.-l.; Jiang, S.; Zhang, J.; Sun, L. First characterization of an anti-lipopolysaccharide factor (ALF) from hydrothermal vent shrimp: Insights into the immune function of deep-sea crustacean ALF. *Dev. Comp. Immunol.* **2018**, *84*, 382–395. [CrossRef]
105. Emani, C.; Garcia, J.M.; Lopata-Finch, E.; Pozo, M.J.; Uribe, P.; Kim, D.-J.; Sunilkumar, G.; Cook, D.R.; Kenerley, C.M.; Rathore, K.S. Enhanced fungal resistance in transgenic cotton expressing an endochitinase gene from *Trichoderma virens*. *Plant Biotechnol. J.* **2003**, *1*, 321–336. [CrossRef] [PubMed]
106. Boot, R.G.; Blommaart, E.F.C.; Swart, E.; der Vlugt, K.G.-V.; Bijl, N.; Moe, C.; Place, A.; Aerts, J. Identification of a Novel Acidic Mammalian Chitinase Distinct from Chitotriosidase. *J. Biol. Chem.* **2001**, *276*, 6770–6778. [CrossRef] [PubMed]
107. Zhu, Z.; Zheng, T.; Homer, R.J.; Kim, Y.-K.; Chen, N.Y.; Cohn, L.; Hamid, Q.; Elias, J.A. Acidic Mammalian Chitinase in Asthmatic Th2 Inflammation and IL-13 Pathway Activation. *Science* **2004**, *304*, 1678–1682. [CrossRef] [PubMed]